JACC: CARDIOVASCULAR IMAGING VOL. 16, NO. 12, 2023

ORIGINAL RESEARCH

Development and Validation of a Prediction Model and Score for Transthyretin Cardiac Amyloidosis Diagnosis

T-Amylo

Xabier Arana-Achaga, MD,[a,b,*] Cristina Goena-Vives, MD,[a,b,c,*] Iñaki Villanueva-Benito, PhD,[a,b] Itziar Solla-Ruiz, MD,[a,b] Ainhoa Rengel Jimenez, MD,[a,b] Teresa Iglesias Gaspar, MD,[d] Iratxe Urreta-Barallobre, MD,[b,d] Gonzalo Barge-Caballero, PhD,[e,f] Sara Seijas-Marcos, PhD,[e] Eva Cabrera, MD,[g] Pablo Garcia-Pavía, PhD,[g,h] María Teresa Basurte Elorz, MD,[i,j] Nerea Mora Ayestarán, MD,[i] Lucas Tojal Sierra, MD,[k] Maria Robledo Iñarritu, MD,[k] Ainara Lozano-Bahamonde, PhD,[l] Vanesa Escolar-Perez, PhD,[l] Cristina Gómez-Ramírez, MD,[m] Elisabete Alzola, MD,[m] Rubén Natividad Andrés, MD,[n] Jose Luis Francisco Matias, MD,[n] Javier Limeres Freire, MD,[o,p,q] Arola Armengou Arxe, PhD,[r] Montserrat Negre Busó, PhD,[s] Jesus Piqueras-Flores, PhD,[t,u] Jorge Martínez-del Río, MD,[t] Jose Juan Onaindia Gandarias, MD,[v] Ibon Rodriguez Sanchez, MD,[v] Ramón Querejeta Iraola, PhD[a,d]

ABSTRACT

BACKGROUND Although transthyretin cardiac amyloidosis (ATTR-CA) is often underdiagnosed, clinical suspicion is essential for early diagnosis.

OBJECTIVES The aim of this study was to develop and validate a feasible prediction model and score to facilitate the diagnosis of ATTR-CA.

METHODS This retrospective multicenter study enrolled consecutive patients who underwent ^{99m}Tc-DPD scintigraphy for suspected ATTR-CA. ATTR-CA was diagnosed if Grade 2 or 3 cardiac uptake was evidenced on ^{99m}Tc-DPD scintigraphy in the absence of a detectable monoclonal component or by demonstration of amyloid by biopsy. A prediction model for ATTR-CA diagnosis was developed in a derivation sample of 227 patients from 2 centers using multivariable logistic regression with clinical, electrocardiography, analytical, and transthoracic echocardiography variables. A simplified score was also created. Both of them were validated in an external cohort (n = 895) from 11 centers.

RESULTS The obtained prediction model combined age, gender, carpal tunnel syndrome, interventricular septum in diastole thickness, and low QRS interval voltages, with an area under the curve (AUC) of 0.92. The score had an AUC of 0.86. Both the T-Amylo prediction model and the score showed a good performance in the validation sample (ie, AUC: 0.84 and 0.82, respectively). They were tested in 3 clinical scenarios of the validation cohort: 1) hypertensive cardiomyopathy (n = 327); 2) severe aortic stenosis (n = 105); and 3) heart failure with preserved ejection fraction (n = 604), all with good diagnostic accuracy.

CONCLUSIONS The T-Amylo is a simple prediction model that improves the prediction of ATTR-CA diagnosis in patients with suspected ATTR-CA. (J Am Coll Cardiol Img 2023;16:1567-1580) © 2023 The Authors. Published by Elsevier on behalf of the American College of Cardiology Foundation. This is an open access article under the CC BY-NC-ND license (http://creativecommons.org/licenses/by-nc-nd/4.0/).

ISSN 1936-878X https://doi.org/10.1016/j.jcmg.2023.05.002

JACC: CARDIOVASCULAR IMAGING, VOL. 16, NO. 12, 2023
DECEMBER 2023:1567–1580

ABBREVIATIONS AND ACRONYMS

^{99m}Tc-DPD = ^{99m}technetium-3,3-diphosphono-1,2 propanodicarboxylic acid

AL-CA = light-chain cardiac amyloidosis

AS = aortic stenosis

ATTR-CA = transthyretin cardiac amyloidosis

CA = cardiac amyloidosis

GLS = global longitudinal strain

HFpEF = heart failure with preserved ejection fraction

IVSd = interventricular septum in diastole

Transthyretin cardiac amyloidosis (ATTR-CA) is a heart disease caused by the deposition of misfolded aggregates of insoluble proteins in the myocardium.[1] There are 2 forms: the hereditary form secondary to pathogenic variants in the transthyretin gene and the wild type (ATTRwt) form, an age-related degenerative process in which there is no variant associated with the disease.

In recent years, scientific interest in ATTR-CA has grown and its diagnosis has improved. On the one hand, technetium-based scintigraphy has become a reliable tool for the noninvasive diagnosis of ATTR-CA, rendering a histological diagnosis unnecessary in most patients.[2,3] In addition to the diagnostic advances, new treatments with promising results in ATTR-CA have been developed, some of which have already shown to be efficacious slowing the disease process.[4] It is thus relevant to identify patients with ATTR-CA who may benefit from the new treatments, especially in the early stages when they are more effective.

The European Society of Cardiology (ESC) Working Group on Myocardial and Pericardial Diseases has proposed to suspect cardiac amyloidosis (CA) in patients with a septum larger than 12 mm in the presence of 1 or more red flags or in special populations, such as heart failure with preserved ejection fraction (HFpEF) and aortic stenosis (AS) in patients over 65 years.[5] In these cases, it is recommended to exclude CA following a diagnostic algorithm based in Tc scintigraphy coupled with exclusion of a monoclonal component in blood and urine. Despite the great advances in cardiac imaging, the diagnosis of CA is frequently delayed or missed,[6,7] partly because of the limited sensitivity and specificity of the red flags alone, the lack of clinical suspicion that is essential for the diagnosis, and the confusion with other diagnoses, such as hypertensive cardiomyopathy and other phenocopies.[6] Applying the guidelines would substantially improve the diagnosis of CA; however, it would also require performing a large amount of ^{99m}technetium-3,3 diphosphono-1,2-propanedicarboxylic acid (DPD) scintigraphies, because the HFpEF and AS population is sizeable. To avoid unnecessary tests, it is thus crucial to improve the screening and suspicion of ATTR-CA, ie, to establish a more precise pretest probability, and to do it in a way that is sustainable from the clinical perspective.

For all of these reasons, the aims of the present study were as follows: 1) to develop a prediction model and a score to predict the diagnosis of ATTR-CA based on widely available clinical, analytical, electrocardiography (ECG), and echocardiographic parameters; 2) to validate them; and 3) to evaluate the performance of both in common clinical scenarios, such as HFpEF, severe AS, and hypertensive cardiomyopathy.

METHODS

This was a retrospective, multicenter, cross-sectional study in 2 steps: development and validation.

DERIVATION AND VALIDATION COHORTS. The derivation cohort included all consecutive patients who had undergone a DPD scintigraphy for suspected

From the [a]Heart Failure and Inherited Cardiac Diseases Unit, Department of Cardiology, Donostia University Hospital, Donostia, Spain; [b]Biodonostia Health Research Institute, Donostia, Spain; [c]Department of Cardiology, Mendaro Hospital, Mendaro, Spain; [d]Clinical Epidemiology Unit, Donostia University Hospital, Donostia, Spain; [e]Heart Failure and Cardiac Transplant Unit, Department of Cardiology, Complexo Hospitalario Universitario A Coruña, Spain; [f]Centro de Investigación Biomédica en Red Enfermedades Cardiovasculares, Instituto de Salud Carlos III, Madrid, Spain; [g]Heart Failure and Inherited Cardiac Diseases Unit, Department of Cardiology, Puerta de Hierro University Hospital, IDIPHISA, CIBERCV, Madrid, Spain; [h]Centro Nacional de Investigaciones Cardiovasculares (CNIC), Madrid, Spain; [i]Department of Cardiology, Navarra University Hospital, Spain; [j]IdiSNA—Health Research Institute of Navarra, Spain; [k]Department of Cardiology, Araba University Hospital-OSI Araba, Spain; [l]Heart Failure Unit, Department of Cardiology, Basurto University Hospital, Bilbao, Spain; [m]Department of Cardiology, Cruces-Barakaldo University Hospital, Bizkaia, Spain; [n]Department of Cardiology, San Eloy Hospital, Bizkaia, Spain; [o]Inherited Cardiac Diseases and Cardiovascular Genetic Unit, Department of Cardiology, Vall de Hebron University Hospital, Barcelona, Spain; [p]Centro de Investigación Biomédica en Red en Enfermedades Cardiovasculares, Madrid, Spain; [q]European Reference Network for Rare and Low Prevalence Complex Diseases of the Heart (ERN GUARD-Heart), Brussels, Belgium; [r]Department of Internal Medicine, Dr Josep Trueta University Hospital, Girona, Spain; [s]Department of Nuclear Medicine, Dr Josep Trueta University Hospital, Girona, Spain; [t]Inherited Cardiac Diseases Unit, Department of Cardiology, Ciudad Real University General Hospital, Ciudad Real, Spain; [u]Facultad de Medicina, University of Castilla la Mancha, Spain; and the [v]Department of Cardiology, Galdakao-Usansolo Hospital, Bizkaia, Spain. *Drs Arana-Achaga and Goena-Vives contributed equally to this paper.

The authors attest they are in compliance with human studies committees and animal welfare regulations of the authors' institutions and Food and Drug Administration guidelines, including patient consent where appropriate. For more information, visit the Author Center.

Manuscript received December 28, 2022; revised manuscript received April 19, 2023, accepted May 1, 2023.

CA from 2016 to 2021. Patients were included if they had interventricular septum in diastole (IVSd) ≥12 mm and at least 1 of the red flags associated with ATTR-CA (listed at the position statement of the ESC Working Group on Myocardial and Pericardial Diseases about the diagnosis and treatment of cardiac amyloidosis).[5] Patients were excluded if the IVSd was <12 mm, the hematological study was not performed despite a positive DPD scan, a biopsy was not carried out when a gammopathy was present, or if a light-chain (AL)-CA could not be ruled out. All of the information was obtained from the electronic health record. The validation cohort included consecutive patients who fulfilled the same inclusion and exclusion criteria mentioned earlier.

For the development of the prediction model (derivation cohort), patients were selected from 2 centers located in the Gipuzkoa region in the north of Spain, the tertiary center Hospital Universitario de Donostia and the regional secondary hospital of Mendaro. The validation cohort was recruited from 11 hospitals across Spain (Complejo Hospitalario A Coruña, Hospital de Basurto, Hospital de Araba, Hospital Universitario Puerta de Hierro Majadahonda, Hospital Universitario de Navarra, Hospital Josep Trueta, Hospital de Ciudad Real, Hospital de Vall de Hebron, Hospital de Cruces, Hospital de Galdakao, and Hospital San Eloy).

The study complied with the Declaration of Helsinki and obtained ethics approval.

CONFIRMATION OF TRANSTHYRETIN CARDIAC AMYLOIDOSIS. ATTR-CA was defined as either the combination of typical imaging features on echocardiography (ie, left ventricular hypertrophy ≥12 mm) with Grade 2 or 3 cardiac uptake on DPD scintigraphy, plus exclusion of clonal dyscrasia—by serum free light-chain (sFLC) assay (Freelite, Binding Site) and serum and urine protein electrophoresis and immunofixation for detecting pathological light chains or a monoclonal component[2]—or, in the presence of a monoclonal gammopathy, a cardiac biopsy containing ATTR amyloid.[5] Cardiac scintigraphy was performed in all patients with 20 mCi of ^{99m}Tc-DPD administered intravenously, taking planar images 3 hours after the administration of the dose. The Perugini grading was used for the qualitative assessment of the images (0 = negative; 1 = inconclusive; 2-3 = positive).[3] No DPD study was performed in the month following a myocardial infarction, and no patient was taking hydroxychloroquine.

The information from the DPD images was collected directly from the departments of nuclear medicine, blinded to the other data collected.

DATA COLLECTION. To construct the models, we collected clinical, echocardiography, and analytical data from the digitized medical records. A detailed list of the variables included and tested is provided in Table 1. Low voltage on the ECG was defined as amplitude of all the QRS complexes of <5 mm in the limb leads and/or <10 mm in the precordial leads. ECG hypertrophy was defined using the Sokolow criteria. Left ventricular ejection fraction was calculated using the Simpson's method, and right ventricular systolic function using tricuspid annular plane systolic excursion.

Strain analysis was performed in the 4-, 3-, and 2-chamber apical views. Global longitudinal strain (GLS) was calculated as the average longitudinal strain (LS) of the 17 segments. Apical sparing was defined as average apical LS/sum of base and mid-LS >1. All other variables were collected as by the medical charts.

STATISTICAL ANALYSIS. Data are presented using summary statistics. Distribution normality was assessed using the Shapiro-Wilk test. To compare patients with and without a confirmed diagnosis of ATTR-CA, the 2-sided Student's *t*-test and chi-square or Fisher exact tests were used, depending on the type of variables.

Prediction model development. Univariable logistic regression model was proposed with all baseline parameters as covariates and the status of ATTR-CA as response variable. Variables showing statistical significance at the 0.1 level were then selected for multivariable logistic regression analysis, along with all variables considered clinically relevant, including the red flags for ATTR-CA diagnosis previously described.[5] Variables with high levels of missingness (>33% missing values) were not included: high sensitivity cardiac troponin T, cardiac magnetic resonance with late gadolinium enhancement pattern, and echocardiographic advanced imaging techniques such as GLS. The intention was to create a pragmatic and parsimonious model, easy to use, and with variables widely available in a routine setting.

To mitigate issues of dimensionality, a least absolute shrinkage and selection operator regression analysis was performed. The variables selected by least absolute shrinkage and selection operator were included in a complete model, and a multiple logistic regression analysis was performed using a backward stepwise selection method to determine the final model.

Internal validation of the final model was carried out using bootstrap with 800 replications to test overfitting. To determine the predictive capacity of

TABLE 1 Baseline Characteristics of the Derivation Sample

	All Patients (N = 227)	No ATTR-CA (n = 119)	ATTR-CA (n = 108)	*P* Value
Age, y	77.3 ± 8.8	75.5 ± 10	79.3 ± 6.7	0.001
Age >80 y	102/227 (44.9)	47/119 (39.5)	55/108 (50.9)	0.08
Male	172/227 (75.8)	72/119 (60.5)	100/108 (92.6)	<0.001
Caucasian	225/227 (99.1)	117/119 (98.3)	108/108 (100)	0.39
Reason for consultation				0.53
Dyspnea	122/217 (56.2)	62/112 (55.4)	60/105 (57.1)	
Extracardiac signs/symptoms	30/217 (13.8)	12/112 (10.7)	18/105 (17.1)	
Arrhythmia/palpitations	10/217 (4.6)	5/112 (4.5)	5/105 (4.8)	
Dizziness/syncope	28/217 (12.9)	18/112 (16.1)	10/105 (9.6)	
Chest pain/angina	12/217 (5.5)	6/112 (5.4)	6/105 (5.7)	
Other	15/217 (6.7)	9/112 (8)	6/105 (5.8)	
Comorbidity				
Arterial hypertension	163/227 (71.8)	89/119 (74.8)	74/108 (65.5)	0.29
Diabetes	56/227 (24.7)	33/119 (27.7)	23/108 (21.3)	0.26
Ischemic heart disease	31/226 (13.7)	16/118 (13.6)	15/108 (13.9)	0.94
HFpEF	115/227 (50.7)	38/119 (31.9)	77/108 (71.3)	<0.001
NYHA functional class				0.22
I	49/227 (21.6)	31/119 (26.1)	18/108 (16.7)	
II	132/227 (58.1)	66/119 (55.5)	66/108 (61.1)	
III-IV	46/227 (20.3)	22/119 (18.5)	24/108 (22.2)	
Permanent pacemaker	33/227 (14.5)	14/119 (11.8)	19/108 (17.6)	0.21
Aortic valve prosthesis	15/226 (6.6)	9/119 (7.6)	6/107 (5.6)	0.56
Ictus	32/227 (14.1)	14/119 (11.8)	18/108 (16.7)	0.29
Chronic kidney disease	49/227 (21.6)	27/119 (22.7)	22/108 (20.4)	0.67
Clinical signs				
Carpal tunnel syndrome	54/227 (23.8)	14/119 (11.8)	40/108 (37)	<0.001
Unilateral	28/227 (12.3)	8/119 (6.7)	20/108 (18.5)	0.007
Bilateral	26/227 (11.5)	6/119 (5)	20/108 (18.5)	0.001
Lumbar canal stenosis	47/227 (20.7)	21/119 (17.6)	26/108 (24.1)	0.23
Peripheral polyneuropathy	19/227 (8.4)	6/119 (5)	13/108 (12)	0.06
Autonomic dysfunction	44/227 (19.4)	19/119 (16)	25/108 (23.1)	0.17
Hypotensive or normotensive, previously hypertensive	40/227 (17.5)	17/119 (14.3)	23/108 (21.3)	0.17
Ruptured biceps tendon	5/227 (2.2)	2/119 (1.7)	3/108 (2.8)	0.57
Cataract	62/227 (27.3)	41/119 (34.5)	21/108 (19.4)	0.01

Continued on the next page

the bootstrap-adjusted model, a receiver-operating characteristic (ROC) curve was generated and the AUC with its 95% CI was calculated. In addition, a locally estimated scatterplot smoothing (LOESS) smoothed calibration curve was drawn, and the slope of the calibration line was determined to evaluate the calibration of the adjusted model.

Simplified score. A simplified diagnostic score was then created as an easy-to-use alternative, not requiring complex equations, online calculators, or mobile applications. Continuous variables were dichotomized using clinically relevant thresholds (ie, IVSd thickness ≥16 mm, which defines severe myocardial hypertrophy). When this was not possible, the diagnostic performance of the variable was tested by calculating its AUC, and the optimal cutoff value was defined as the point with the highest sum of sensitivity and specificity (ie, age ≥80 years). The regression coefficients of the final model became the weights of each parameter. Each point was obtained considering the lowest coefficient as the unit, with each weight allocated based on the obtained coefficient rounded to the nearest integer. For simplicity purposes, once the punctuation score was obtained, the punctuation was modified while accounting for the proportional weight of each coefficient, yielding a modified score.

Cutoffs. Cutoff points were established in both the prediction model and score, to classify patients into 3 risk groups according to the probability of being diagnosed with ATTR-CA: low risk, intermediate risk,

TABLE 1 Continued

	All Patients (N = 227)	No ATTR-CA (n = 119)	ATTR-CA (n = 108)	*P* Value
Electrocardiographic parameters				
First-degree AV block	36/221 (16.3)	13/114 (11.4)	23/107 (21.5)	0.04
Atrial fibrillation/flutter	119/227 (52.4)	52/119 (43.7)	67/108 (62)	0.006
LBBB	25/224 (11.2)	11/117 (9.4)	14/107 (13.1)	0.38
RBBB	36/224 (15.2)	14/117 (12)	20/107 (18.7)	0.16
Low QRS voltage	50/224 (22.3)	12/117 (10.3)	38/107 (35.5)	<0.001
Pseudo-infarct pattern	87/224 (38.8)	34/117 (29.1)	53/107 (49.5)	0.002
Hypertrophy pattern	61/223 (27.4)	42/116 (36.2)	19/107 (17.8)	0.002
Echocardiographic parameters				
IVSd, mm	16.6 ± 3.3	15.4 ± 2.9	18 ± 3.3	<0.001
Severe hypertrophy (IVS ≥16 mm)	125/227 (55.1)	44/119 (37)	81/108 (75)	<0.001
LVEDD, mm	46.8 ± 6.8	47.5 ± 7.2	46.1 ± 6.4	0.14
PWT, mm	15.1 ± 3.1	13.8 ± 2.9	16 ± 3	<0.001
LVEF, %	55.8 ± 11.3	56.3 ± 11.7	55.2 ± 10.8	0.47
LVEF <50%	47/225 (20.1)	22/117 (18.8)	25/108 (23.1)	0.42
E/e′	15.9 ± 7.4	14 ± 6.4	17.6 ± 7.8	0.002
E/e′ >15	80/163 (49.1)	29/76 (38.2)	52/89 (58.4)	0.009
Diastolic pattern grade >2	27/216 (12.5)	8/111 (7.2)	19/105 (18.1)	0.016
LA volume, mL	49.3 ± 18.8	51 ± 22	48 ± 16	0.32
LA dilation	204/219 (93.2)	102/112 (91.1)	102/107 (95.3)	0.21
Aortic stenosis	47/226 (20.8)	30/118 (25.4)	17/108 (15.7)	0.07
Pulmonary hypertension (>50 mm Hg)	29/223 (13)	13/116 (11.2)	16/107 (15)	0.41
TAPSE, mm	18.5 ± 5.4	20.9 ± 5.6	17 ± 4.8	<0.001
Right ventricular hypertrophy	30/224 (13.4)	8/116 (6.9)	22/108 (20.4)	0.003
Pericardial effusion	15/224 (6.7)	7/116 (6.1)	8/108 (7.4)	0.50
LV global longitudinal strain[a]	−12.7 ± 4.8	−14 ± 4.9	−11.9 ± 4.6	0.04
Apical sparing[a]	57/100 (57)	14/42 (33.3)	43/58 (74.1)	<0.001
CMR performed[a]	60/227 (26.2)	24/119 (20.2)	36/108 (32.7)	0.03
Presence of LGE	42/60 (70)	10/24 (41.7)	32/36 (88.9)	<0.001
Diffuse subendocardial pattern	18/60 (30)	2/10 (20)	16/32 (50)	<0.001
Laboratory values				
NT-proBNP, pg/mL	1,666 (579-3,953)	1,416 (309-3,133)	2,208 (944-4,530)	0.94
NT-proBNP >1,800 pg/mL	96/199 (48.2)	40/97 (41.2)	56/102 (54.9)	0.05
Clinical HF or NT-proBNP >1,800 pg/mL	148/203 (72.9)	54/97 (55.7)	94/106 (88.5)	<0.001
Creatinine, mg/dL	1.3 ± 1.2	1.4 ± 1.5	1.2 ± 0.4	0.07
eGFR, mL/min	64.6 ± 22.9	65.1 ± 25.8	64 ± 19.3	0.73
eGFR <60 mL/min	78/224 (34.8)	39/118 (33.1)	39/106 (36.8)	0.56
Hs troponin T, ng/mL	70.7 ± 162	72 ± 240	70 ± 53	0.94
Hs troponin T >40 ng/mL	51/95 (53.5)	12/41 (29.3)	39/54 (72.2)	<0.001

Values are mean ± SD, n/N (%), or median (IQR). **Bold** indicates the red flags of the guidelines and their prevalence in our study. [a]Global longitudinal strain and CMR performed in limited subset of patients.

ATTR-CA = transthyretin cardiac amyloidosis; AV = atrioventricular; CMR = cardiovascular magnetic resonance; E/e′ = e-wave/e′-wave ratio; eGFR = estimated glomerular filtration rate; HF = heart failure; HFpEF = heart failure with preserved ejection fraction; Hs = high-sensitivity; IVS = interventricular septum; IVSd = interventricular septum in diastole; LA = left atrial; LBBB = left bundle branch block; LGE = late gadolinium enhancement; LV = left ventricular; LVEDD = left ventricular end-diastolic diameter; LVEF = left ventricular ejection fraction; NT-proBNP = N-terminal pro-brain natriuretic peptide; PWT = posterior wall thickness; RBBB = right bundle branch block; TAPSE = tricuspid annular plane systolic excursion.

and high risk. The primary aim of the different cutoffs provided was to avoid misdiagnosis of cardiac amyloidosis. These cutoffs were established based on the highest sensitivity (low-moderate) and highest specificity (moderate-high) (Table 2).

Validation. Both the prediction model and score were then tested in the validation cohort. The AUC was calculated to evaluate its discriminative ability, and a calibration plot was constructed to evaluate its calibration.

In addition, in the validation cohort 3 subgroups were defined: 1) patients with diagnosis of severe AS; 2) patients with diagnosis of HFpEF defined by ESC guidelines; and 3) patients with hypertensive cardiomyopathy, considered if previous diagnosis of hypertension was made and the interventricular

TABLE 2 Diagnostic Accuracy of Different Cutoffs of the Simplified Score for the Diagnosis of Transthyretin Cardiac Amyloidosis in Derivation and Validation Cohorts

	Derivation Cohort (n = 224)						Validation Cohort (n = 895)					
T-Amylo Score	Sensitivity	Specificity	FP	FN	TP	TN	Sensitivity	Specificity	FP	FN	TP	TN
≥0	100 (99-100)	0	117 (52)	0 (0)	107 (48)	0 (0)	100 (99-100)	0	499 (56)	0 (0)	396 (44)	0 (0)
≥1	100 (99-100)	9 (3-15)	106 (47)	0 (0)	107 (48)	11(5)	99 (98-100)	9 (8-9)	454 (51)	5 (1)	391 (44)	45 (5)
≥2	100 (99-100)	23 (15-31)	90 (40)	0 (0)	107 (48)	27 (12)	97 (96-99)	23 (23-24)	382 (43)	10 (1)	386 (43)	117 (13)
≥3	99 (97-100)	27 (19-35)	85 (38)	1 (1)	106 (47)	32 (14)	94 (92-97)	34 (33-35)	328 (37)	22 (3)	374 (42)	171 (19)
≥4	94 (90-99)	54 (45-63)	54 (24)	6 (3)	101 (45)	63 (28)	84 (80-88)	61 (58-63)	197 (22)	63 (7)	333 (37)	302 (34)
≥5	88 (82-94)	63 (55-72)	43 (19)	13 (6)	94 (42)	74 (33)	78 (74-82)	70 (67-73)	150 (17)	88 (10)	308 (34)	349 (39)
≥6	73 (64-81)	82 (75-89)	21 (9)	29 (13)	78 (35)	96 (43)	62 (58-67)	86 (82-91)	68 (8)	149 (17)	247 (28)	431 (48)
≥7	48 (38-57)	94 (90-98)	7 (3)	56 (25)	51 (23)	110 (49)	34 (30-39)	96 (90-100)	19 (2)	260 (29)	136 (15)	480 (54)
≥8	36 (26-46)	96 (92-99)	5 (2)	68 (30)	39 (17)	112 (50)	27 (22-31)	98 (92-100)	9 (1)	291 (33)	105 (12)	490 (55)
≥9	11 (5-17)	100 (99-100)	0 (0)	95 (42)	12 (5)	117 (52)	13 (9-16)	99 (92-100)	3 (1)	346 (39)	50 (6)	496 (55)
≥10	7 (2-12)	100 (99-100)	0 (0)	99 (44)	8 (4)	117 (52)	5 (2-7)	99 (92-100)	1 (1)	378 (42)	18 (2)	498 (56)
≥11	4 (1-7)	100 (99-100)	0 (0)	103 (46)	4 (2)	117 (52)	2 (1-3)	100 (92-100)	0 (0)	388 (43)	8 (1)	499 (56)

Values are median (25th-75th percentile) or n (%).
FN = false negative; FP = false positive; TN, true negative; TP = true positive.

septum was ≥12 mm before de DPD scan was performed.

Due to the small number of missing data in the variables included in the prediction model (only 3 cases in one variable in the derivation cohort and no missing data in the validation cohort), a complete case analysis was performed.

In addition, an external validation of the Mayo Clinic ATTR-CA score[8] was performed among patients with HFpEF in the derivation cohort (n = 114). Discrimination and calibration were evaluated with the AUC and Hosmer-Lemeshow goodness-of-fit test respectively.

Analyses were performed at the 2-tailed significance level of $P < 0.05$, using Stata version 16 (StataCorp).

RESULTS

DERIVATION COHORT. From a total of 254 DPD scintigraphy studies, 6 patients were excluded because IVSd was <12 mm, so the eligible population included 248 patients. Among the DPD-positive group (n = 129), 17 patients were excluded because no complete hematological study had been performed, and 4 were excluded because it was not possible to rule out a light-chain cardiac amyloidosis (AL-CA) and a biopsy was not performed.

Of the 227 patients included, 108 (48%) had positive DPD scintigraphy (Grade 2-3 uptake) and met the diagnostic criteria of ATTR-CA, and 119 (52%) were DPD-negative (115 patients with Grade 0 uptake and 4 with Grade 1 uptake) (Figure 1). Among the DPD-positive patients, 12 (9.3%) had either monoclonal gammopathy or free light chain elevation. ATTR was confirmed by endomyocardial biopsy in 3 of them. Although 5 patients had free light-chain elevation, AL-CA was excluded because a normal serum free light chain sFLC ratio with no monoclonal component was confirmed. Of those with ATTR-CA, 90% underwent a genetic study by complete sequencing of the TTR gene: 90 presented the ATTRwt form and 8 had pathogenic variants in the TTR gene (all p.Val50Met).

Baseline characteristics of the cohort are shown in Table 1. Patients with ATTR-CA were more frequently men and older and had a greater incidence of carpal tunnel syndrome and HFpEF than those without ATTR-CA. Regarding ECG features, atrial fibrillation, first-degree atrioventricular block, low voltages, and pseudo-infarct pattern were more frequent in the ATTR-CA group, whereas ECG criteria of left ventricular hypertrophy were more prevalent in the negative DPD-group. A greater IVSd thickness, worse diastolic dysfunction, and more severe tricuspid annular plane systolic excursion reduction were observed in the ATTR-CA group. Regarding strain parameters, the ATTR-CA group showed worse GLS and more frequent systolic apex-to-base sparing pattern ratio.

PREDICTIVE MODEL DEVELOPMENT: THE T-AMYLO PREDICTION MODEL. The variables included in the final multivariable analysis were age, gender, carpal tunnel syndrome, lumbar spinal stenosis, IVSd thickness, low QRS interval voltage, Q waves, permanent pacemaker, first-degree atrioventricular block, right bundle branch block, atrial fibrillation/flutter, and N-terminal pro-B-type natriuretic peptide. Table 3 shows the diagnostic value of each variable in the derivation cohort.

FIGURE 1 **Flow Diagram of Patients in the Derivation Cohort**

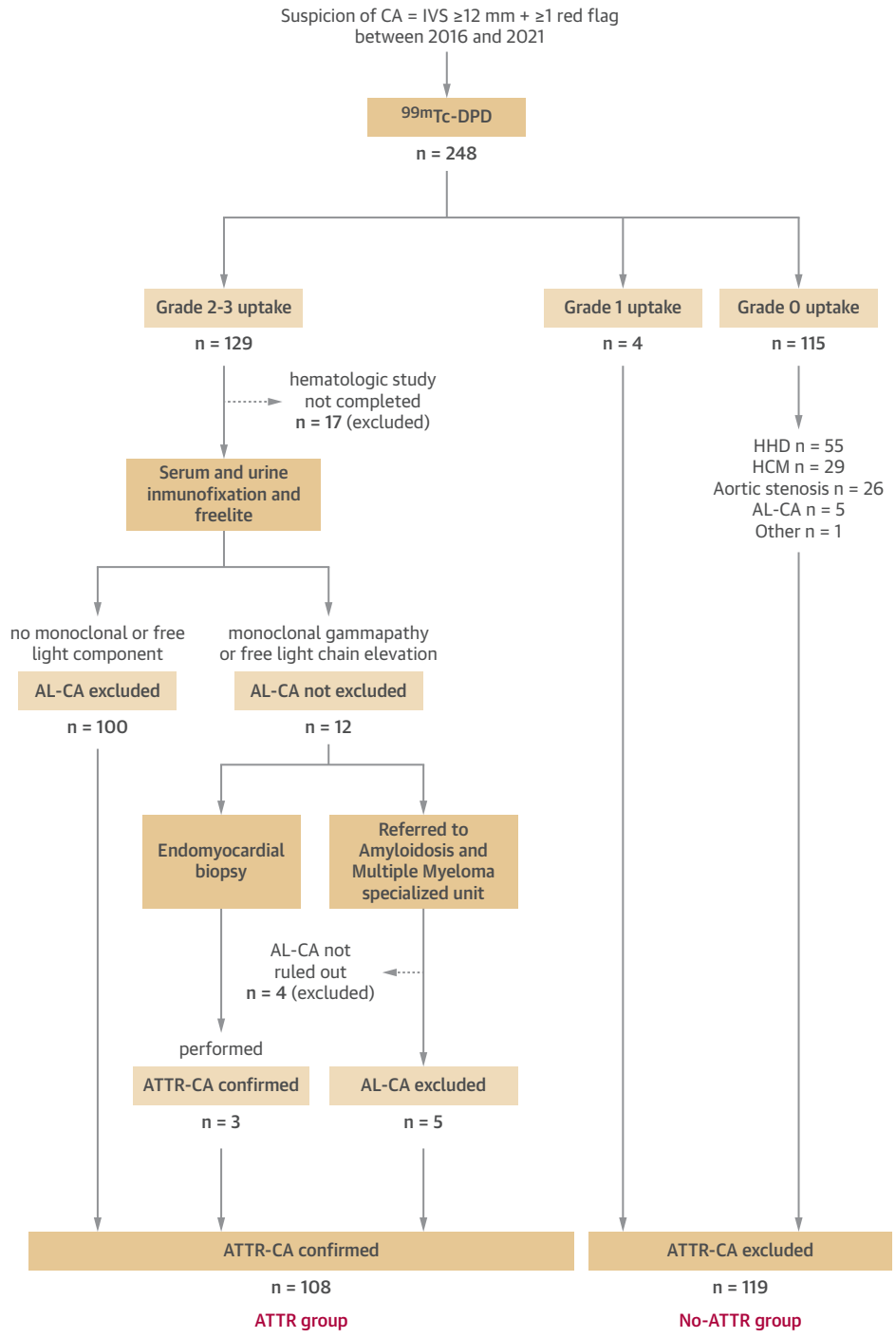

Patients who underwent a ^{99m}technetium-3,3-diphosphono-1,2 propanodicarboxylic acid (^{99m}Tc-DPD) scintigraphy for suspected cardiac amyloidosis (interventricular septum in diastole [IVSd] ≥12 mm and a red flag) were included. If Perugini grade 2 to 3 and no monoclonal component was observed, they were classified as transthyretin cardiac amyloidosis (ATTR-CA) confirmed (ATTR group). If Perugini grade 0 to 1 was observed they were classified as ATTR-CA excluded (no-ATTR group). If the hematological study was not performed despite a positive DPD scan or if light-chain cardiac amyloidosis (AL-CA) could not be ruled out, patients were excluded.

TABLE 3 Diagnostic Accuracy of the Variables Proposed for Multivariable Analysis

	AUC	95% CI	Cutoff	Sensitivity	Specificity	PPV	NPV
Age, y	0.60	0.53-0.67	80	51	61	58	54
Male	0.66	0.59-0.73		40	93	86	58
Carpal tunnel syndrome	0.63	0.55-0.70		37	88	74	61
Lumbar spinal stenosis	0.53	0.46-0.61		24	82	55	54
Pseudo-infarct pattern	0.60	0.53-0.68		50	71	61	61
Low QRS voltage	0.63	0.55-0.70		36	90	76	60
First-degree AV block	0.55	0.47-0.63		22	89	64	55
IVSd, mm	0.75	0.69-0.82	16	63	75	65	73
Permanent pacemaker	0.53	0.45-0.61		18	88	58	54
RBBB	0.53	0.46-0.61		19	88	59	54
Atrial fibrillation/flutter	0.59	0.52-0.67		56	62	56	62
NT-proBNP	0.61	0.53-0.69	1,800	55	59	58	55

AUC = area under the receiver-operating characteristic curve; NPV = negative predictive value; PPV = positive predictive value; other abbreviations as in Table 1.

The final prediction model (T-Amylo) included age, gender, carpal tunnel syndrome, IVSd thickness, and low QRS interval voltage, which showed the best diagnostic accuracy (Figure 2, Table 4). The apparent AUC was 0.92 (95% CI: 0.88-0.95); the bootstrap-corrected AUC was 0.89 (95% CI: 0.85-0.93) with bootstrap shrinkage = 0.932.

Based on the T-Amylo prediction model, patients can be classified into low, intermediate, and high probability of an ATTR-CA diagnosis (Central Illustration). In the derivation sample, 29% of the patients were in the low-risk group, among which only 3% had a confirmed ATTR-CA.

T-AMYLO SCORE. A simplified scoring model was obtained assigning points as follows (Table 4): 1 point for age ≥80 years, 2 points for IVSd thickness ≥16 mm, 2 points for low QRS interval voltage, 3 points for male gender, and 3 points for carpal tunnel syndrome. The final score ranged from 0 to 11. The simplified scoring model had a diagnostic performance of AUC: 0.86 (95% CI: 0.81-0.90) (Figure 2).

Table 2 shows the diagnostic accuracy of different cutoffs of the T-Amylo score for the diagnosis of ATTR-CA in the derivation and validation cohorts. The selected cutoffs produced 3 risk groups according to the probability of being diagnosed with ATTR-CA: 0 to 2 points (low risk), 3 to 6 points (intermediate risk), and 7 to 11 points (high risk) (Central Illustration).

VALIDATION. The validation cohort included 895 patients, of whom 396 (44.2%) had a positive DPD and 499 (55.8%) a negative one. Patient characteristics are displayed in Supplemental Table 1.

In the validation cohort, the T-Amylo prediction model showed an AUC of 0.84 (95% CI: 0.82-0.87) (Figure 2). Remarkably, the AUCs were >0.79 in all hospitals (Supplemental Table 2). The T-Amylo score showed an AUC of 0.82 (95% CI: 0.79-0.85). A total of 25% of the patients from the validation cohort were classified as low risk with a sensitivity of 95% and specificity of 41% (Supplemental Table 3).

The Mayo ATTR-CM score validated in our derivation sample HFpEF population (n = 114) showed a good prediction accuracy (AUC: 0.80 [95% CI: 0.72-0.89]; Hosmer-Lemeshow *P* value = 0.44) (Figure 3).

T-AMYLO PERFORMANCE ACCORDING TO CLINICAL SCENARIOS. The diagnostic performance of the T-Amylo prediction model was optimal in the 3 subgroups: hypertensive cardiomyopathy (n = 327), (AUC: 0.89 [95% CI: 0.86-0.93]); severe AS (n = 105) (AUC: 0.85 [95% CI: 0.77-0.93]); and HFpEF (n = 604) (AUC: 0.86 [95% CI: 0.83-0.88]) (Figure 4, Supplemental Table 4). The T-Amylo score also showed a good diagnostic performance in these subgroups (Figure 4). Supplemental Table 3 shows diagnostic accuracies of the prediction model and the score in validation cohort and in these 3 clinical scenarios.

DISCUSSION

We herein present the T-Amylo prediction model with excellent diagnostic performance to detect patients with ATTR-CA. This regression formula includes a combination of easily available clinical, ECG, and echocardiographic variables that can classify patients with suspected ATTR-CA more precisely than the recommended red flags. This model was developed in a representative multicenter sample and validated in another large cohort in 11 centers. The best diagnostic accuracy was obtained from a

FIGURE 2 **Discrimination and Calibration of the T-Amylo Prediction Model/Score**

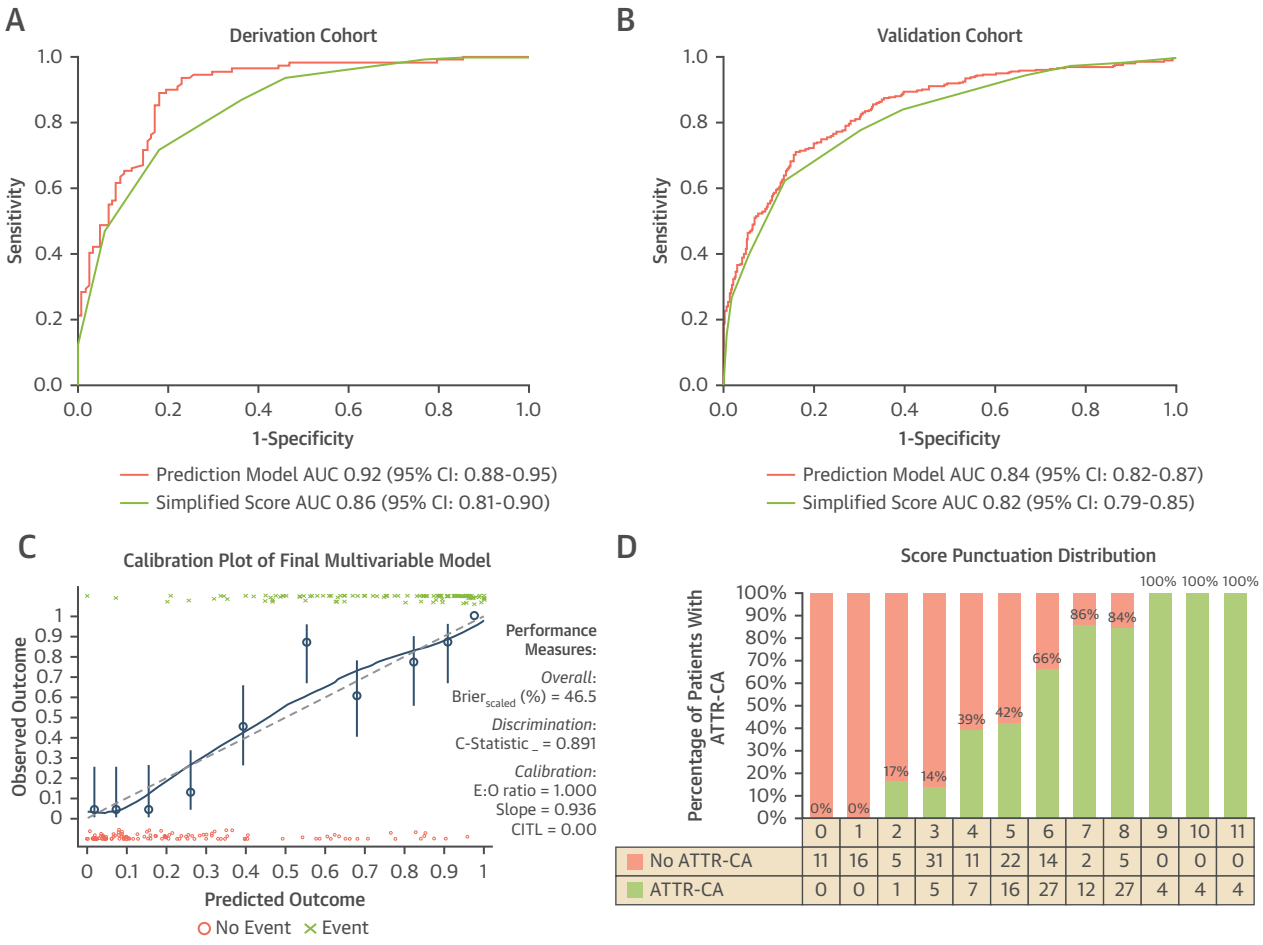

Receiver-operating characteristic curves showing an excellent discrimination for both the final multivariable prediction model (red curve) and the simplified score (blue curve) in the derivation cohort (A) and validation cohort (B). Internal validation of the model by bootstrapping (C) showed very good agreement between predicted (x-axis) and observed (y-axis) events (ATTR-CA). Blue circles represent binned logistic regression estimates with 95% confidence for deciles of the predicted outcome. The dashed diagonal line represents the line of perfect calibration, and the solid blue line the continuous calibration (hazard regression). Red crosses reflect the number of patients with ATTR-CA with a predicted diagnosis corresponding to the x-axis value, and green circles the number of patients without ATTR-CA with a predicted diagnosis corresponding to the x-axis value. (D) The percentage of ATTR-CA (black bars) across the distribution of T-Amylo simplified score punctuation. AUC = area under the curve; other abbreviations as in Figure 1.

combination of age, male sex, previous carpal tunnel syndrome, IVSd thickness, and low voltages. Moreover, we simplified the model (T-Amylo score) while maintaining good accuracy. Finally, both showed good performance in the subgroups where ATTR-CA is more prevalent.

Our study is the first to analyze a combination of clinical, ECG, analytical, and echocardiographic variables for the specific diagnosis of ATTR-CA. The Mayo Clinic has recently published a score to identify patients at high risk of presenting ATTR-CA in the population with HFpEF who have undergone DPD.[8] The ATTR-CM score showed a good prediction accuracy in our HFpEF population. However, there are differences between both scores. On the one hand, the Mayo group score applicability is reduced to a single clinical scenario such as HFpEF, whereas the T-Amylo score is universally applicable once the suspicion of ATTR has been established. On the other hand, the 2 cutoff strategies used in the T-Amylo score improve both the positive and, more important, the negative predictive value (Figure 3). Finally, the ATTR-CM score is based mainly on echocardiographic variables and does not take into account high

TABLE 4 Independent Diagnostic Variables From the Multivariable Analysis and Diagnostic Score

	OR	Regression Coefficient	95% CI	*P* Value	T-Amylo Scoring
Final Multivariable Formula					
Carpal tunnel syndrome	21.087	3.049	(1.924-4.173)	0.000	
Male	15.371	2.732	(1.605-3.860)	0.000	
IVSd (1 mm)	1.394	0.332	(0.191-0.472)	0.000	
Low QRS interval voltage	3.487	2.013	(1.022-3.005)	0.000	
Age (1 y)	1.183	0.168	(0.104-0.232)	0.000	
Constant		−21.941		0.000	
Simplified Scoring Model					
Carpal tunnel syndrome	8.401	2.128	(1.239-3.017)	0.000	3
Male	8.852	2.181	(1.223-3.138)	0.000	3
IVSd (mm) (≥16)	5.792	1.756	(1.039-2.473)	0.000	2
Low QRS interval voltage	5.199	1.648	(0.773-2.523)	0.000	2
Age (y) ≥80 y	3.553	1.268	(0.526-2.009)	0.001	1
Constant		−4.243		0.000	

Abbreviation as in Table 1.

prevalence red flags such as carpal tunnel syndrome, whereas the T-Amylo score also includes clinical and ECG features which may improve the prediction capacity. It is well known that the carpal tunnel syndrome is a prognostic marker in ATTR-CA, regardless of cardiac involvement, and precedes the diagnosis of CA by 5 to 9 years.[9,10] The association of carpal tunnel syndrome with other ECG and echocardiographic variables presents high diagnostic accuracy and could be used for early diagnosis. Variables of diastolic dysfunction or the GLS and apical sparing are associated with myocardial amyloid infiltration, and they have high diagnostic capacity,[11,12] as supported by our data. Noteworthy, a multiparametric echocardiographic score has demonstrated good diagnostic accuracy,[10] but it is based on strain parameters that are not readily available in the cardiology clinic or are difficult to obtain because of poor acoustic windows, geriatric population, and so on. For this reason, we aimed to create a simple prediction model/score with accessible, widely available variables, easy to remember and interpretate, that does not require advanced cardiac imaging parameters (eg, GLS or cardiac magnetic resonance), and that any physician could use, from primary care to specialist consultation. To maintain greater diagnostic precision, we recommend using the prediction model (see the online calculator[13] or the QR code in the **Central Illustration**).

The diagnosis of ATTR-CA can be very challenging. The ESC Working Group on Myocardial and Pericardial Diseases position paper has proposed to suspect and screen for CA in patients with a left ventricular wall thickness ≥12 mm in the presence of ≥1 red flags or special populations (HFpEF and severe AS in patients >65 years). However, many of the red flags are nonspecific and also appear in the general population without the presence of amyloidosis. Moreover, HFpEF and severe AS populations are sizeable, which entails a risk of excessive scintigraphy tests, unnecessary radiation, overload of nuclear medicine and hematology departments, and so on. For all of these reasons, we propose using the T-Amylo prediction model/score in 2 different scenarios. First, it could be useful when ATTR-CA is suspected based on guidelines (LV wall thickness ≥12 mm and presence of some red flags/clinical scenarios), in which case it would serve to exclude those patients in whom the diagnosis of ATTR-CA is very unlikely (around 30%) without the need of additional tests (**Central Illustration**). Second, the T-Amylo prediction model/score could be used in patients age >65 years with hypertrophic phenotype and previously diagnosed HFpEF, severe AS, or hypertensive cardiomyopathy (**Figure 4**). Previous studies have shown that ATTR-CA is frequent in elderly patients admitted with HFpEF,[14,15] in those with severe AS,[9,16,17] and in those previously misdiagnosed with hypertensive cardiomyopathy.[6-12,14-18] The application of the T-Amylo prediction model/score may increase recognition of ATTR-CA and it may contribute to earlier diagnosis, which increases the likelihood that patients will benefit from the new treatments. With the current availability of effective targeted treatments, the correct diagnosis of ATTR-CA is crucial. With this in mind, the purpose of the selected cutoff points is to guide noninvasive diagnosis in a cost-effective way, and it may be used to guide DPD scintigraphy. In that sense, one of the greatest values of the T-Amylo prediction model/score is to know whom not to test with DPD with excellent reliability (negative predictive value of 97% for both the model and the score). Therefore, we propose to apply an online calculator to predict ATTR-CA risk: when the result obtained reflects a high risk of ATTR-CA, confirmation with scintigraphy along with exclusion of monoclonal component is mandatory. However, when the risk of ATTR-CA is low, we suggest that clinicians not perform DPD because ATTR-CA is very unlikely and reconsider the differential diagnosis of hypertrophic phenotype. In the intermediate group, the diagnosis of ATTR-CA is possible, and we thus suggest reconsidering other red flags and using the multiparametric echocardiographic score as an additional aid in the diagnosis of ATTR-CA. If clinical suspicion persists, we recommend performing tests to diagnose ATTR-CA.

CENTRAL ILLUSTRATION **Proposed Diagnostic Algorithm Using the T-Amylo Prediction Model/Score**

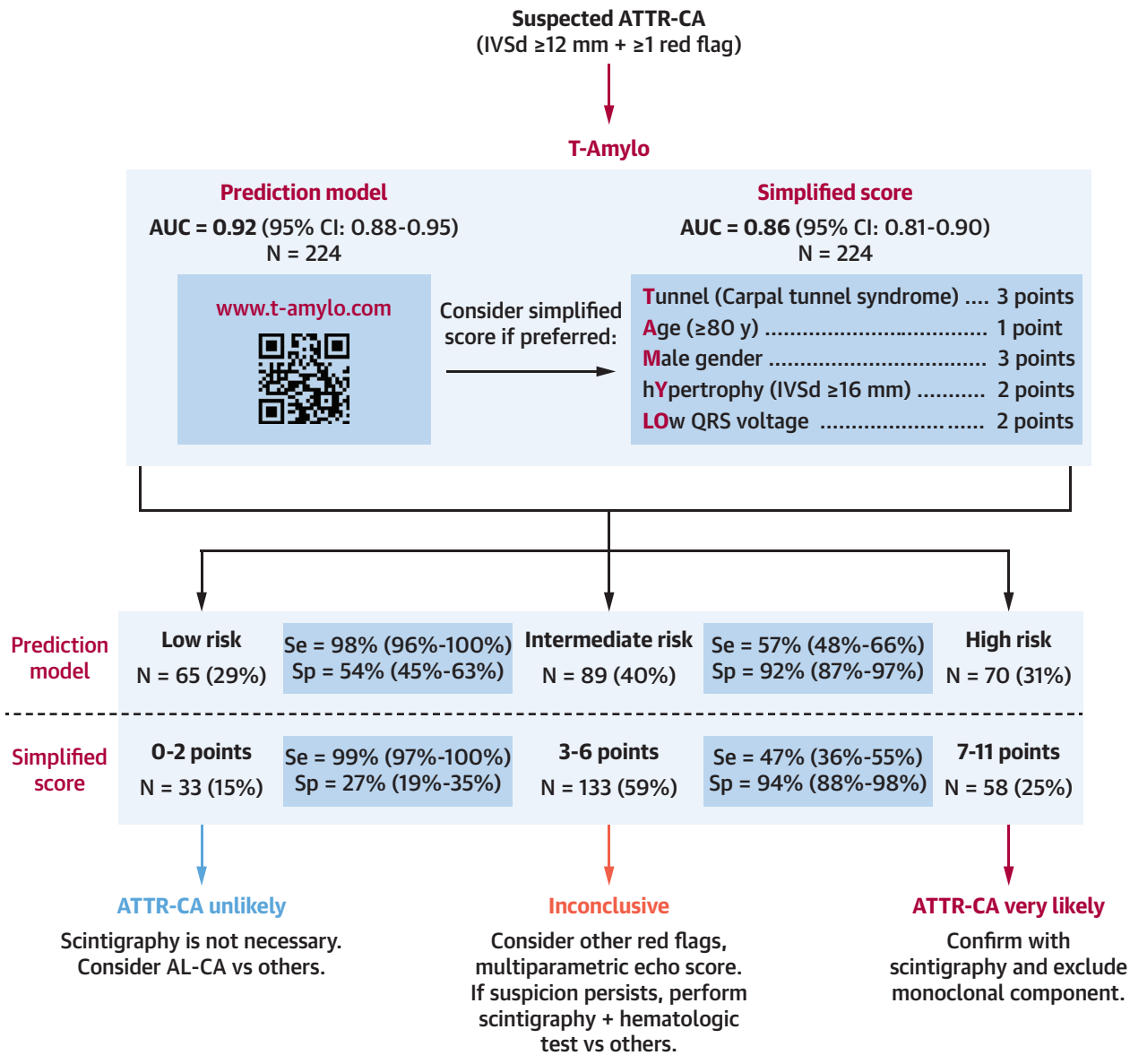

Arana-Achaga X, et al. J Am Coll Cardiol Img. 2023;16(12):1567–1580.

The clinical suspicion diagnosis based on the predictive value of the T-Amylo. Highly specific cutoffs prioritize patients who should undergo noninvasive diagnosis confirmation of transthyretin cardiac amyloidosis, whereas highly sensitive cutoffs could reasonably exclude it without the need for further imaging tests. AL-CA = light-chain cardiac amyloidosis; ATTR-CA = transthyretin cardiac amyloidosis; AUC = area under the curve; IVSd = interventricular septum in diastole; Se = sensitivity; Sp = specificity.

STUDY LIMITATIONS. This study presents the limitations inherent to any retrospective study, subject to selection and measurement biases. Our study population was very heterogeneous, except for the fact that all patients were Caucasian, and the clinical suspicion and indication of DPD scintigraphy could vary according to the centers; however, the T-Amylo showed optimal accuracy in all centers. We are also aware that some red flags associated with high diagnostic suspicion may have not been correctly assessed because it is a retrospective study. Variables, such as traumatic rupture of the biceps, right

FIGURE 3 Comparison of ATTR-CM Score and T-Amylo Score in HFpEF Population

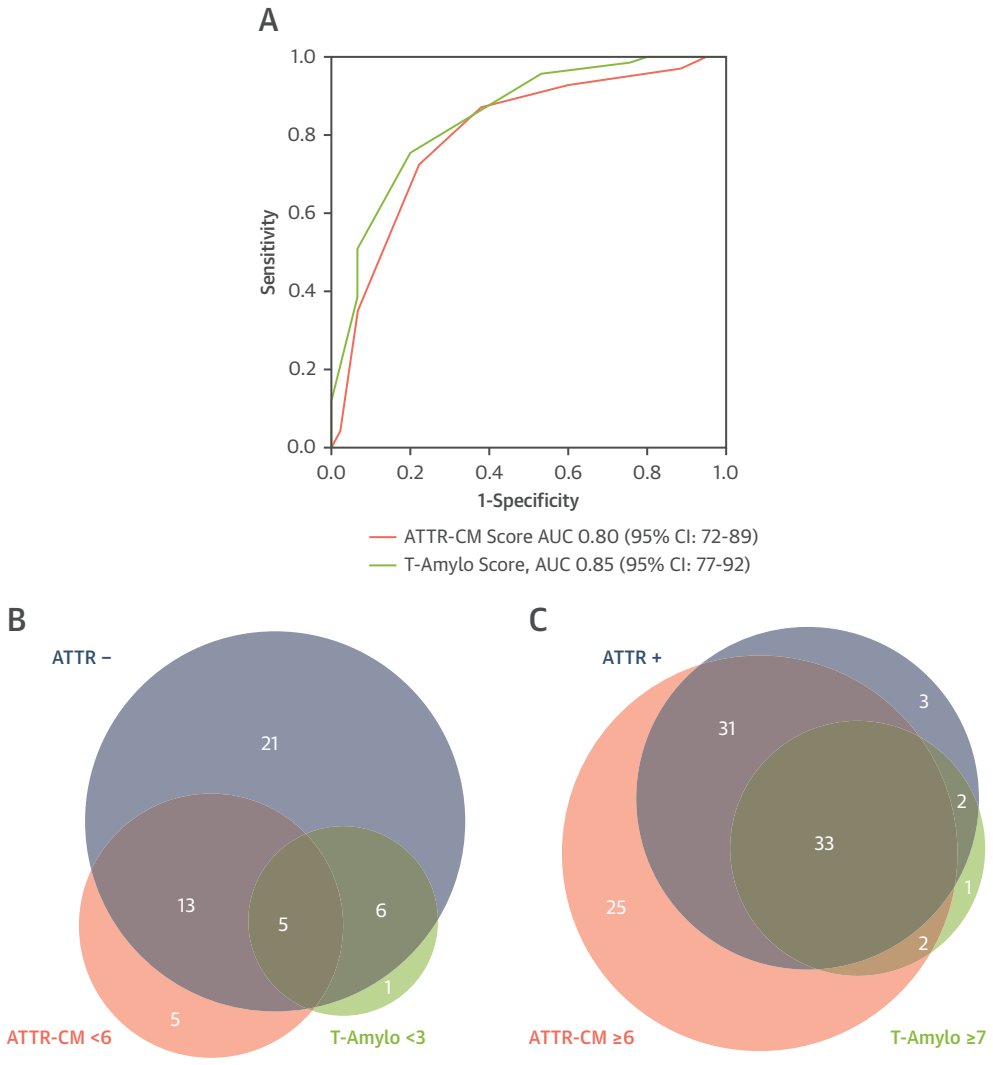

(A) Receiver-operating characteristic curves showing the AUC of ATTR-CM score (red curve) and the T-Amylo score (blue curve) in HFpEF patients. Venn diagrams showing the number of patients screened out (B) and screened in (C) with ATTR-CM score (red circles) and T-AMYLO score (blue circles). With the 2 different cutoffs strategy in the T-AMYLO score, the number of false positives (FP) and false negatives (FN) are substantially reduced. HFpEF = heart failure with preserved ejection fraction; other abbreviations as in **Figure 1**.

ventricular hypertrophy, or poor tolerance to or hypotension induced by heart failure drugs, are probably important red flags that may have a greater predictive value prospectively. In particular, the low prevalence of biceps tendon rupture in our series compared with other series[19] reflects the difficulty of collecting this variable retrospectively. In addition, diastolic dysfunction variables and strain parameters are not included in the score. Seven patients presented concomitant monoclonal gammopathy, and although complete hematological study excluded AL-CA, cardiac biopsy demonstrating transthyretin was not performed. As only 8 patients had TTR allelic variant (all Val30Met), this would limit the generalizability of results to the wild-type ATTR-CA. A recently published study has focused on the diagnosis of ATTR-CA in HFpEF patients without left ventricular hypertrophy,[20] but in our study, we did not consider that option and strictly adhered to guidelines. Similarly, the score is not valid for the diagnosis of AL-CA. Finally, the association of obesity to low voltages and tunnel carpal syndrome might reduce

FIGURE 4 Proposed Screening of Transthyretin Cardiac Amyloidosis in High-Prevalence Clinical Scenario

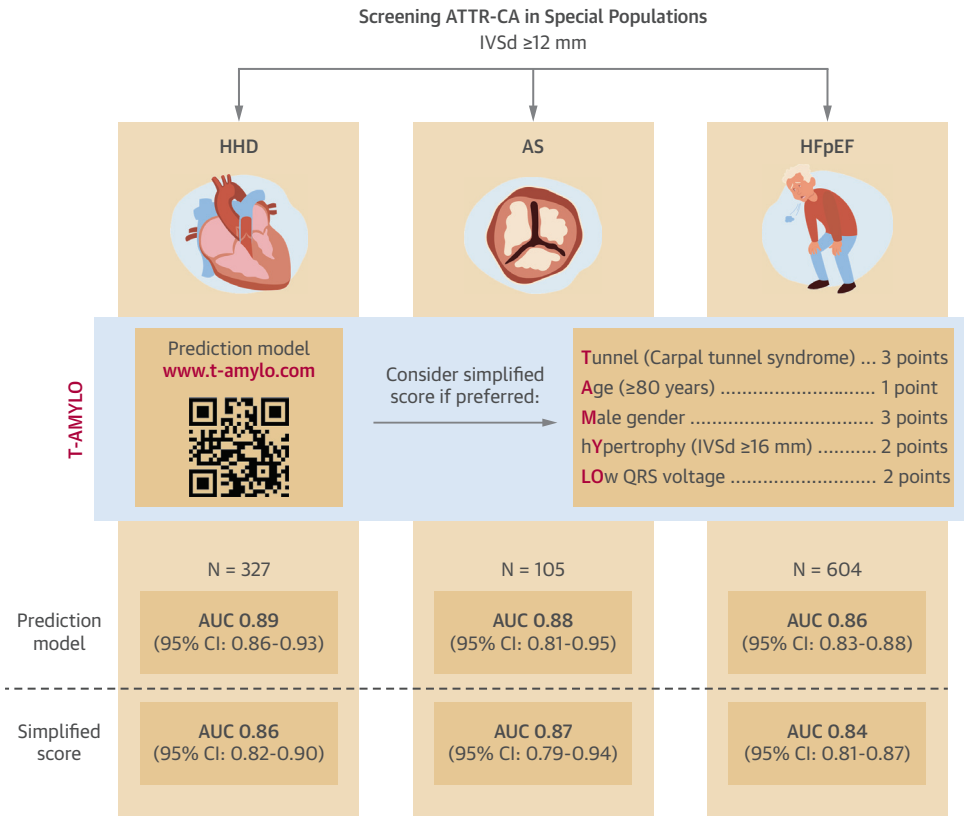

Hypertensive heart disease (HHD), aortic stenosis (AS), and HFpEF are 3 clinical scenarios in which transthyretin cardiac amyloidosis should be ruled out/confirmed to achieve specific diagnosis. The T-Amylo score shows a good predictive value in this subgroup. Abbreviation as in Figure 3.

the specificity of the score in an obese population. Although we believe that the T-Amylo is applicable when ATTR-CA is suspected, prospective studies are required to validate our results and confirm our assumption.

CONCLUSIONS

The diagnosis of ATTR-CA has significantly improved in recent years as a result of the emergence of noninvasive diagnosis. Yet, the condition is still underdiagnosed, and high clinical suspicion is required. Here, we propose a feasible prediction model/score, based on simple and widely available parameters that any physician can easily use in patients with LV hypertrophy to increase the likelihood of ATTR-CA and, therefore, prioritize patients who should undergo ATTR-CA noninvasive diagnosis confirmation. By using highly sensitive cutoffs, ATTR-CA could be reasonably excluded in around 30% of patients with left ventricular hypertrophy without the need for further imaging tests.

FUNDING SUPPORT AND AUTHOR DISCLOSURES

Part of this project was funded by Pfizer through an independent general research grant (number 64764667). This study has been partially funded by Instituto de Salud Carlos III through the project "PI20/01379" (co-funded by European Regional Development Fund/ European Social Fund "A way to make Europe"/"Investing in your future"). The CNIC is supported by the ISCIII, MCIN, the Pro-CNIC Foundation, and the Severo Ochoa grant (CEX2020-001041-S). Dr Basurte Elorz has received a consultant fee from Pfizer. All other authors have reported that they have no relationships relevant to the contents of this paper to disclose.

ADDRESS FOR CORRESPONDENCE: Dr Xabier Arana-Achaga, Paseo Dr Beguiristain S/N 20014, Donostia Gipuzkoa, Spain. E-mail: xabier.aranaachaga@osakidetza.eus. OR Dr Cristina Goena-Vives, Paseo Dr Beguiristain S/N 20014, Donostia Gipuzkoa, Spain. E-mail: crisgoena@gmail.com. @crisgoena.

PERSPECTIVES

COMPETENCY IN PATIENT CARE AND PROCEDURAL SKILLS: The combination of easily available variables of the T-Amylo prediction model/score may help the physicians in nonspecialized amyloidosis centers in the suspicion diagnostic process of transthyretin cardiac amyloidosis, making it more rational and simpler.

TRANSLATIONAL OUTLOOK: The main fields of development of this diagnostic tool would be, on the one hand, the prospective evaluation of its predictive value in different ethnicities and clinical scenarios, and on the other hand, the capacity to achieve earlier diagnosis by enabling access to specific prognosis-modifying treatments.

REFERENCES

1. Nitsche C, Scully PR, Patel KP, et al. Prevalence and outcomes of concomitant aortic stenosis and cardiac amyloidosis. *J Am Coll Cardiol*. 2021;77:128–139.

2. Gillmore JD, Maurer MS, Falk RH, et al. Nonbiopsy diagnosis of cardiac transthyretin amyloidosis. *Circulation*. 2016;133:2404–2412.

3. Perugini E, Guidalotti PL, Salvi F, et al. Noninvasive etiologic diagnosis of cardiac amyloidosis using 99mTc-3,3-diphosphono-1,2-propanodicarboxylic acid scintigraphy. *J Am Coll Cardiol*. 2005;46:1076–1084.

4. Maurer MS, Schwartz JH, Gundapaneni B, et al. Tafamidis treatment for patients with transthyretin amyloid cardiomyopathy. *N Engl J Med*. 2018;379:1007–1016.

5. Garcia-Pavia P, Rapezzi C, Adler Y, et al. Diagnosis and treatment of cardiac amyloidosis: a position statement of the ESC Working Group on Myocardial and Pericardial Diseases. *Eur Heart J*. 2021;42:1554–1568.

6. Lopez-Sainz A, Hernandez-Hernandez A, Gonzalez-Lopez E, et al. Clinical profile and outcome of cardiac amyloidosis in a Spanish referral center. *Rev Esp Cardiol (Engl Ed)*. 2021;74:149–158.

7. Bishop E, Brown EE, Fajardo J, et al. Seven factors predict a delayed diagnosis of cardiac amyloidosis. *Amyloid*. 2018;25:174–179.

8. Davies DR, Redfield MM, Scott CG, et al. A simple score to identify increased risk of transthyretin amyloid cardiomyopathy in heart failure with preserved ejection fraction. *JAMA Cardiol*. 2022;7:1036–1044.

9. Itzhaki Ben Zadok O, Abelow A, Vaxman I, et al. Prior carpal tunnel syndrome and early concomitant echocardiographic findings among patients with cardiac amyloidosis. *J Card Fail*. 2020;26:909–916.

10. Milandri A, Farioli A, Gagliardi C, et al. Carpal tunnel syndrome in cardiac amyloidosis: implications for early diagnosis and prognostic role across the spectrum of aetiologies. *Eur J Heart Fail*. 2020;22:507–515.

11. Boldrini M, Cappelli F, Chacko L, et al. Multiparametric echocardiography scores for the diagnosis of cardiac amyloidosis. *J Am Coll Cardiol Img*. 2020;13:909–920.

12. Nicol M, Baudet M, Brun S, et al. Diagnostic score of cardiac involvement in AL amyloidosis. *Eur Heart J Cardiovasc Imaging*. 2020;21:542–548.

13. A red flag transthyretin cardiac amyloidosis risk prediction model. T-AMYLO. Accessed June 6, 2023. www.t-amylo.com

14. Gonzalez-Lopez E, Gallego-Delgado M, Guzzo-Merello G, et al. Wild-type transthyretin amyloidosis as a cause of heart failure with preserved ejection fraction. *Eur Heart J*. 2015;36:2585–2594.

15. Hahn VS, Yanek LR, Vaishnav J, et al. Endomyocardial biopsy characterization of heart failure with preserved ejection fraction and prevalence of cardiac amyloidosis. *J Am Coll Cardiol HF*. 2020;8:712–724.

16. Castano A, Narotsky DL, Hamid N, et al. Unveiling transthyretin cardiac amyloidosis and its predictors among elderly patients with severe aortic stenosis undergoing transcatheter aortic valve replacement. *Eur Heart J*. 2017;38:2879–2887.

17. Scully PR, Patel KP, Treibel TA, et al. Prevalence and outcome of dual aortic stenosis and cardiac amyloid pathology in patients referred for transcatheter aortic valve implantation. *Eur Heart J*. 2020;41:2759–2767.

18. Gonzalez-Lopez E, Gagliardi C, Dominguez F, et al. Clinical characteristics of wild-type transthyretin cardiac amyloidosis: disproving myths. *Eur Heart J*. 2017;38:1895–1904.

19. Hallie I Geller, Danielle Trota, Rodney H Falk, et al. Ruptured biceps tendon: a novel non-cardiac clue to TTR cardiac amyloidosis. *Circulation*. 2015;132:A12716.

20. Devesa A, Camblor Blasco A, Pello Lazaro AM, et al. Prevalence of transthyretin amyloidosis in patients with heart failure and no left ventricular hypertrophy. *ESC Heart Fail*. 2021;8:2856–2865.

KEY WORDS amyloidosis, prediction model, suspicion diagnosis, transthyretin

APPENDIX For supplemental tables, please see the online version of this paper.